

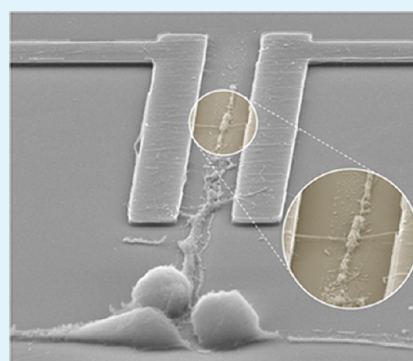
Highly Ordered Large-Scale Neuronal Networks of Individual Cells – Toward Single Cell to 3D Nanowire Intracellular Interfaces

Moria Kwiat,[†] Roey Elnathan,[†] Alexander Pevzner,[†] Asher Peretz,[‡] Boaz Barak,[§] Hagit Peretz,[†] Tamir Ducobni,[†] Daniel Stein,[†] Leonid Mittelman,[‡] Uri Ashery,[§] and Fernando Patolsky^{*,†}

[†]School of Chemistry, The Raymond and Beverly Sackler Faculty of Exact Sciences, [‡]Department of Physiology, Sackler Medical School, and [§]Department of Neurobiology, The George S. Wise Faculty of Life Sciences, School of Neuroscience, Tel Aviv University, Tel Aviv 69978, Israel

S Supporting Information

ABSTRACT: The use of artificial, prepatterned neuronal networks in vitro is a promising approach for studying the development and dynamics of small neural systems in order to understand the basic functionality of neurons and later on of the brain. The present work presents a high fidelity and robust procedure for controlling neuronal growth on substrates such as silicon wafers and glass, enabling us to obtain mature and durable neural networks of individual cells at designed geometries. It offers several advantages compared to other related techniques that have been reported in recent years mainly because of its high yield and reproducibility. The procedure is based on surface chemistry that allows the formation of functional, tailor-made neural architectures with a micrometer high-resolution partition, that has the ability to promote or repel cells attachment. The main achievements of this work are deemed to be the creation of a large scale neuronal network at low density down to individual cells, that develop intact typical neurites and synapses without any glia-supportive cells straight from the plating stage and with a relatively long term survival rate, up to 4 weeks. An important application of this method is its use on 3D nanopillars and 3D nanowire-device arrays, enabling not only the cell bodies, but also their neurites to be positioned directly on electrical devices and grow with registration to the recording elements underneath.



KEYWORDS: neuron, cellular network, electrophysiology, nanowires, chemical pattern

INTRODUCTION

Developing new methods and technologies for patterning neurons into artificial networks is a useful tool for addressing fundamental questions in the field of neurobiology.¹ The culturing of cells on prepatterned surfaces, compared to natural environment, allows fabrication of simpler networks, which might be better suited for studying the basic interactions between cells, allowing highly defined experiments to be performed concerning cellular interactions, network behavior, pharmaceutical testing, and the development of neurochips and biosensors.^{2–5} Most approaches employed to understand the activity of neuronal networks in vitro make use of dissociated neuronal cell cultures.⁶ However, the random spatial distribution and overlap of neurons, neurites and glia cells complicate the observation of single neuron.⁷ In early studies, survival was obtained only in high density systems⁸ whereas neurons did not survive in low density cultures.⁶ Nevertheless, studies have shown that hippocampal and cortical neurons can be maintained healthy in serum free conditions for several weeks at low densities cultures of neurons,^{9,10} but still, current techniques do not perform consistently when it comes to single cell scale. On the other hand, directed neuronal growth in which cell soma and neurites are constrained to a prescribed pattern obviates these difficulties and enables the study of individual neurons and their interactions during the develop-

ment of the network. Hence, considerable efforts have been made for creating patterned cellular circuits of individual cells.¹¹

Several methods were developed throughout the years for surface patterning and control of neuronal attachment and growth. Most of which involve microcontact printing,^{12–17} lithography,^{8,18,19} or laser and UV ablation of proteins, amino acids, and amino silanes.^{20–23} For the most part, those methods were developed for silicon and glass-based substrates, but with proper modifications were also adapted for planar electrode arrays. Planar microelectrode arrays (MEAs)^{24,25} offer the advantage of long term, simultaneous, extracellular recording of electrical activity from multiple locations of a network where the recorded signals are action potentials from neurons in close proximity to the electrodes.²³ Specifically for these purposes, patterning is highly important because of two major drawbacks that make MEAs less than ideal for the study of network function: very low signal to noise ratio that is partially caused by the imprecise positioning of electrodes relative to the cell,^{26,27} and glia cells that often occlude electrodes from detecting neuronal activity.²³ Especially in the presence of serum, glia cells are abundant and form a carpet like structure²⁸

Received: April 6, 2012

Accepted: June 12, 2012

Published: June 22, 2012

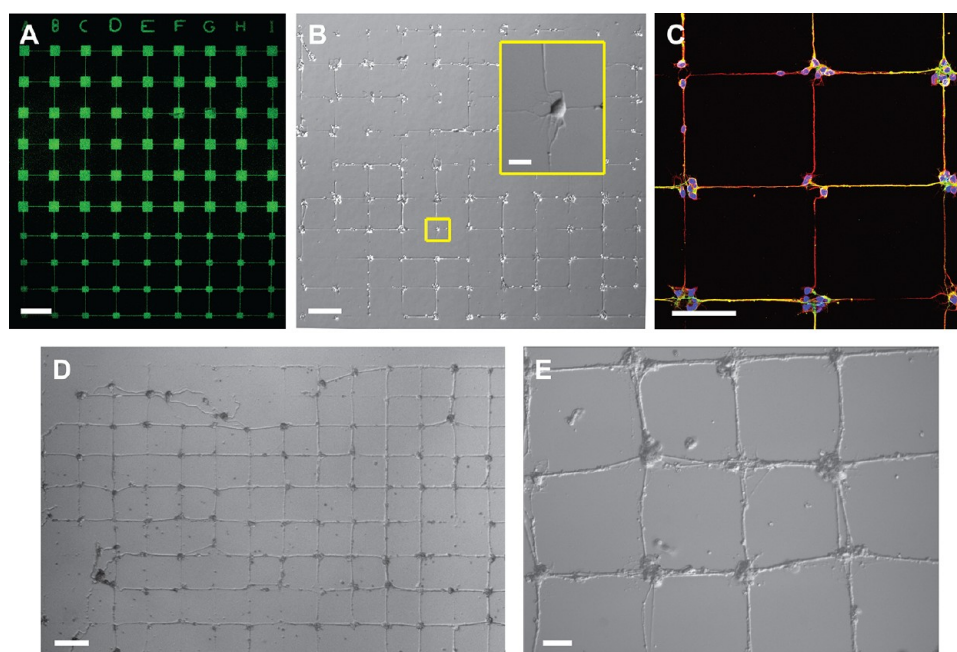


Figure 1. Optical and confocal images of cortical neuronal network glia-free cultured on chemically pre-patterned Si wafer designed as linear network. (A) Fluorescent image of photolithography-defined pattern of FITC-bounded poly-L-lysine for cells attachment of $50/30\ \mu\text{m}$ width squares and $2 \times 100\ \mu\text{m}$ width \times length interconnecting lines. Scale bar is $100\ \mu\text{m}$. (B–C) Images of 3 day old living network grown according to the chemical pattern in A. B inset shows a magnification of the boxed cell. Scales bar are 100 and $10\ \mu\text{m}$, respectively. (C) Confocal microscope image of the network. Each labeled cell body corresponds to labeled axons and dendrites, indicating the growth of solely neurons without any glia cells. Dendrites are labeled with MAP-2 (red), axons labeled with TAU (green) and nucleus labeled with DAPI (blue). Scale bar is $75\ \mu\text{m}$. (D, E) 2 weeks old cortical neuronal network. The network successfully maintains its geometry almost without the collapse of cells into the flourosilane area. (E) Magnification of image D. Scale bars are $100\ \mu\text{m}$ and $25\ \mu\text{m}$, respectively.

which shields the electrical transfer between neurons and substrates;¹⁷ but also in serum-free medium it was reported that glia density is significantly elevated for patterned cultures.²⁹ Rarely, each electrode has only a single neuron growing atop; it generally has either no neurons or a cluster of neurons.³⁰ Therefore, the use of extracellular electrodes is limited to the recording of field potentials generated by action potentials^{31,32} and only in rare instances can synchronized synaptic potentials in highly ordered neuronal networks be picked up by extracellular electrodes.^{33,34} With a goal of individual neurons located at each electrode site, this inefficiency for functional recording sites may be an obstacle for optimal electrical MEA use.

In addition, electrical recording of small mammalian neurons, which are particularly relevant for the investigation of neurological diseases, is harder to achieve in comparison to large invertebrate neurons because of their relative small signals.³⁵ Also, the interfacing electrodes have to be sufficiently small, often in the order of individual cell body, to isolate signals from a single neuron while disregarding the activity of nearby cells.²⁷ Fabrication of biosensors that match mammalian neuronal sizes has become possible thanks to the miniaturization of microelectronics. Nevertheless, the ability to create state-of-the-art transistors that have sufficiently low noise level for neuron-electronic interfacing is not enough; these individual elements need also to be addressed in a precise manner with the neuron cells to increase the contact area.

Whereas many existing methods are capable of producing patterns suitable for neurons, there has yet been no simple reliable method to simultaneously provide high-resolution

patterns with high compliance of cells to desired patterns with good manufacturability and long shelf life.³⁶

We have therefore established a simple yet robust protocol for confining the growth of cortical and hippocampal neuronal cells alongside their axons and dendrites into ordered and defined architectures, creating artificial pre-patterned design. It fulfills essential and non trivial requirements such as low cell density of neurons culture without any glia supportive cells straight from the plating stage, and persistent survival on the growth pattern for long term, until mature and functional synapses are formed. The presented procedure is applied for controlling neuronal growth on silicon wafers and polished glasses, as well as on 3D nanopillars and 3D Si nanowires (NWs) electrical devices, allowing us to obtain mature and durable networks of single cells at precise geometries.

RESULTS AND DISCUSSION

Neuron cell growth can be guided by using various chemically adhesive and repelling factors.^{15,17,36,37} To attain more effective cell patterning, cell repellant material is sometimes established alongside the cell's adhesive micropatterns to further enforce the compliance of cells and their processes to the desired patterns, and later on to prevent them from wandering. Microcontact printing for instance, often does not provide an explicit cell repellant material to help enforce compliance, though more recent developments have incorporated such provisions.³⁶ Although previous works have demonstrated the creation of individual neuronal networks,^{15,19} our method exhibits significantly improved fidelity and reproducibility. Here, we describe a procedure that combines surface chemistry and a single step of photolithography in which polylysine

patterns confine the adhesion of cellular bodies to prescribed 30–50 μm width squares and the neuritic growth to thin 2 μm width lines, surrounded by a repelling the fluorosilane layer (Figure 1A). The surface chemistry is based on spontaneous chemisorption and physisorption through self organization of the functional groups (fluorosilane and polylysine, respectively), with a thickness of approximately 2–4 nm, which allows the functionalization of silicon oxide surfaces. In this regard, the formation of a tight, highly thin interface between the neurons and the substrate is especially promising for the monitoring and/or stimulation of neurons by electrodes, as the weak coupling between them due to the extracellular cleft is one of the major problems in neuron–electronic interfaces.³⁸ First, the substrate surfaces are coated with a hydrophobic fluorosilane self assembled monolayer (SAM), followed by a photolithography step that defines the micro-pattern; then fluorosilane layer is peeled from the exposed pattern-region by a plasma treatment, and finally, polylysine is added, rendering the pattern region to hydrophilic (see Figure S1 in the Supporting Information). Critical to the success of our method is tuning the surface coverage of the fluorosilane layer to a level of hydrophobicity that would not disrupt the following photolithography step. The fluorosilane surface coverage can be tuned by altering the solvent type, water content, deposition time, and temperature.³⁹

This strategy enabled us to produce artificial neuronal networks that were maintained at low densities, down to single cells, on Si wafers and polished glasses (Figure 1). Cortical and hippocampal rat neurons, 99.9% glia-free (provided as fresh micro-surgically dissected tissue from Genlantis Inc.), have been successfully cultured and developed with intact neuronal physiology up to 3–4 weeks in defined and highly ordered large-scale networks. We have deliberately excluded glia cells from our system as these would potentially compromise the stated goal of our work to grow solely electrically-active neuronal cells. On average, about 1–3 cells were settled in each square (Figure 2) and developed neurites according to the interconnecting lines. The viability of the cells was evaluated during their

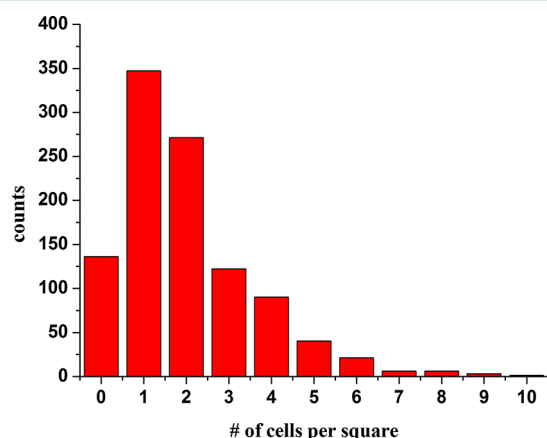


Figure 2. Image describes how many cell bodies are settled in a square. The distribution of the number of cells confined in a 50 μm width square is presented. A total amount of 1043 squares was collected out of 27 patterned wafers with living cells, taken from 7 independent experiments conducted at different timing, that were prepared under the very same conditions. This data illustrates that the average number of cells per square is 1.77, with 33% of the squares containing a single cell.

growth based on their morphology and neurite extension. Furthermore, immunocytochemistry studies with typical common markers as Tau and MAP2 for axons and dendrites, and Synaptophysin for synapses⁴⁰ revealed that the network exhibits normal morphology and development. Immunostaining with GFAP showed negligibly detectable staining, confirming the absence of glia cells in the culture. In addition, electrophysiology studies of the network using a whole-cell configuration of the patch-clamp technique exhibited evoked and spontaneous electrical activity (Figure 3) in accordance with other studies that have shown that electrophysiological properties of neurons grown on patterned substrates are similar to those observed in classical “random” low-density cultures.^{19,29}

We were able to overcome the low survival rate that is naturally accompanied to low cell densities and the absence of glia by applying a sandwich configuration for the cells growth with a glass slide on top of the cells, thus reducing the oxygen concentration to physiological levels.^{9,10}

The primary limitation of our method lies in its relatively lower survival duration in comparison to months of maintenance with the presence of glia-cells, although we did witness glia-free networks that lasted over a month. Nevertheless, its achievements fulfill great importance that we deem it to be better suited to trace the behavior of individual neurons with a relatively low cell density and a short culture time.

These properties of a network could be of interest to studies that investigate basic neurobiology and systematic screening of new pharmacological compounds by using a wide variety of patterns that can be designed to form auto-synapses (autapses), linear networks or other matrices. Furthermore, a principle design goal can be used for electrochemical detection by using cells positioned directly adjacent to microfabricated electrodes, ensuring that transmitter molecules released from a synapse or a portion of the cell surface adjacent to the electrode are rapidly and completely oxidized.⁴¹

Another important application of such a network is its implementation on nanowire (NW) based neuron devices which have been recently noted for their great potential in neuroscience. Many approaches can be utilized for the fabrication of NW-based neuron devices, including coupling NW transistors to neurons^{42,43} and probing neurons with vertical NW arrays.^{44,45} Studies have shown that the native SiO_2 layer of SiNWs comes into substantial contact with neurons and that neuronal processes are attached tightly to the SiNWs, forming omega-shaped interfaces with highly thin interfacial layers.³⁸ This coupling may be advantageous for the development of neuron devices in terms of signal transfer and electronic coupling.

In recent years a number of studies at the interface of nanotechnology and cell biology have shown that vertically aligned NWs support cell attachment and survival.^{46–52} Moreover, vertical electrodes were used to record both extracellular and intracellular action potentials of cells such as cardiomyocytes.^{53,54} Intracellular recordings and stimulation of individual *Aplysia* neurons were also recently demonstrated⁵⁵ by nail shaped structures, however cortical mammalian cells cultured on these chips failed to engulf them and in most cases died after 2 days. Another prominent obstacle mentioned by Spira was the competition of glia cells over the engulfment of the electrodes.³⁴ In a different study, cortical rat neurons were indeed shown to grow on vertical nanopillars with a tendency of the cell membrane to wrap around the nanopillars.³⁰ Another

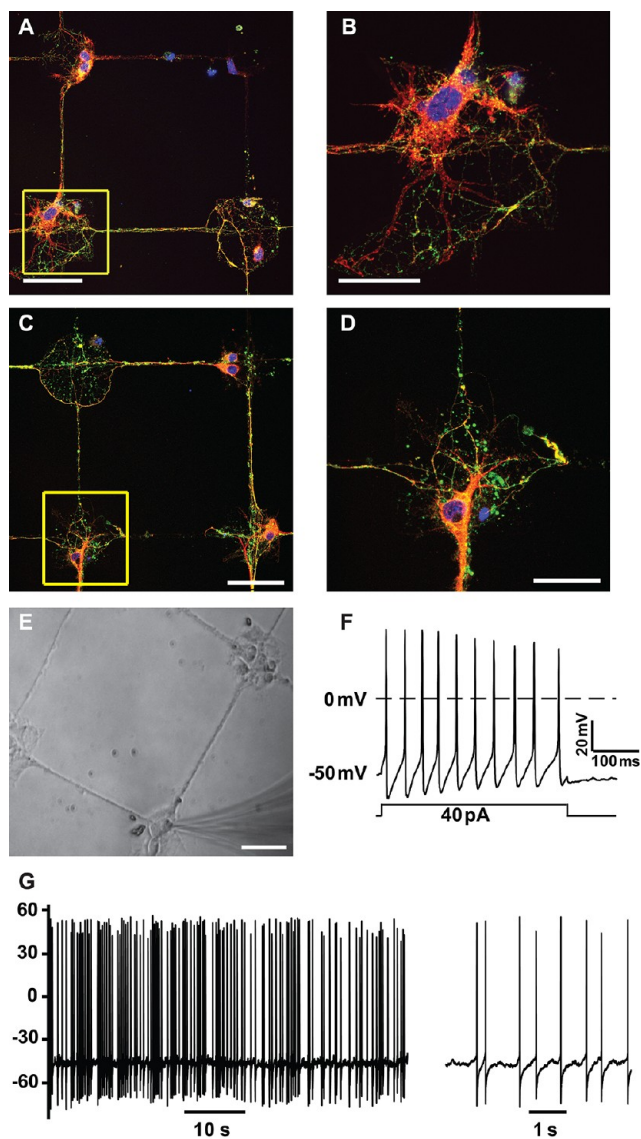


Figure 3. Immunocytochemistry and electrophysiology exhibit mature and electrically active network. (A, B) Confocal microscope images of 7 day old network exhibiting neurites growth and typical cell morphology. Dendrites are labeled with MAP-2 (red), axons labeled with TAU (green) and nucleus labeled with DAPI (blue). (B) Magnification of the cell boxed in (A). Scale bars are 75 and 25 μm , respectively. (C, D) Confocal microscope images of 10 day old cortical cells labeled with MAP-2 for dendrites (red), Synaptophysin for synapses (green) and DAPI for nucleus (blue). Synaptophysin-immunostaining is distributed in clusters, suggesting that synapses are spread all over the network. Scale bars are 50 μm and 25 μm , respectively. (D) Magnification of the cell boxed in (C). (E–G) Patch-clamp electrical recording of 9 day old hippocampal network exhibiting evoked and spontaneous synaptic currents. (E) Optical image of the neuronal network and the patch pipette. Scale bar is 50 μm . (F) Evoked spiking activity by a square depolarizing current pulse (40 pA for 400 ms) using the whole cell configuration. (G) Spontaneous neuronal activity with 10 seconds (left panel) and 1 second (right panel) time scales.

important work demonstrated a scalable intracellular electrode platform based on vertical Si nanowires that allowed electrical interfacing to rat cortical neurons.⁵⁶ Although it provides a clear path towards simultaneous, high fidelity interfacing with hundreds of individual neurons, it lacks the ability to access

axons and dendrites in a deliberate and precise manner since it deals with dissociated cultures. In that regard, a NW-based device that penetrates intentionally to the cell neurites rather than to the soma and measures intracellular signals for periods of days will be an unprecedented achievement. For that purpose, our controlled neurons growth method can be used to provide the essential tools for such outstanding challenges.

As a proof-of-concept, we have grown vertical Si nanopillars of 70–100 nm diameter and 1 μm height that are spaced 4 μm apart in a pattern of squares and lines that were chemically modified with fluorosilane and polylysine, as described, according to their pattern. Cortical neuronal rat cells, glia free, were successfully grown on the pillars according to their pattern with pillars in tight contact not only with the cell body of individual cells, but also with the neurite projections, creating a highly ordered and durable network (Figure 4). Cells survived for at least 14 days on these pillars presenting intact neuronal physiology and mature synapses as illustrated by their labeling with MAP2 and Synaptophysin (see Figure S2 in the Supporting Information). We were able to position the cells directly on the pillars and grow the neurite projections in registration to the pillars underneath.

Potentially, each nanopillar, as an intracellular electrode, would be able to detect signals not only from a single neuron, but also from axons and dendrites spatially located along the pillars array. These highly local and noninvasive nano-probes of neuronal projections may offer significant advantages over conventional electrophysiological methods that can measure intracellular potentials with decent spatial resolution; as well, such probes could be used for local chemical sensing along the neurites, a capability that the other technologies still cannot offer.

Lastly, our procedure to confine neuronal growth was implemented on 3D suspended SiNW field-effect transistor (FET) devices. A prerequisite for local extracellular probing of neural excitation is an adequate sensitivity of sufficiently small analog microelectronic devices in an aqueous environment.³⁵ The basic idea in transistor recording is that the neuron is directly attached to the exposed gate oxide of a FET. During an action potential, current flows through the adhering cell membrane and along the cleft between the chip and the cell, and changes the electrical field of the gate, which results in direct modulation of the source-drain conductance. Transistors with large gate area yield a low noise level, but the chances for a good neuron-gate match are low. Therefore, it is advantageous to use smaller transistors despite their higher noise levels. For that reason, nanowires can be used as unique probes for neurons, allowing a subtle interaction with the cell with ultra-high sensitivity. The small diameters and high performance of the nanowires yield highly sensitive devices, which have been noted for their detection ability of single molecules and the local extracellular activity of neuronal excitation.⁵¹

Many efforts are devoted to increasing the area of the neuron-sensor junction in an attempt to improve the low cell resistance formed between the plasma membrane and the electronic device.^{55,57} The main approaches are based on: chemical functionalization of the substrate on which the neurons grow through molecules that promote stronger adhesion,^{58,59} on altering the surface topography on which the neurons grow,^{60,61} or to locally increase the surface area (by using carbon nanotubes for example^{62,63}). We were therefore challenged to improve the effective electrical coupling by applying our protocol on 3D-SiNWs-based FET devices,

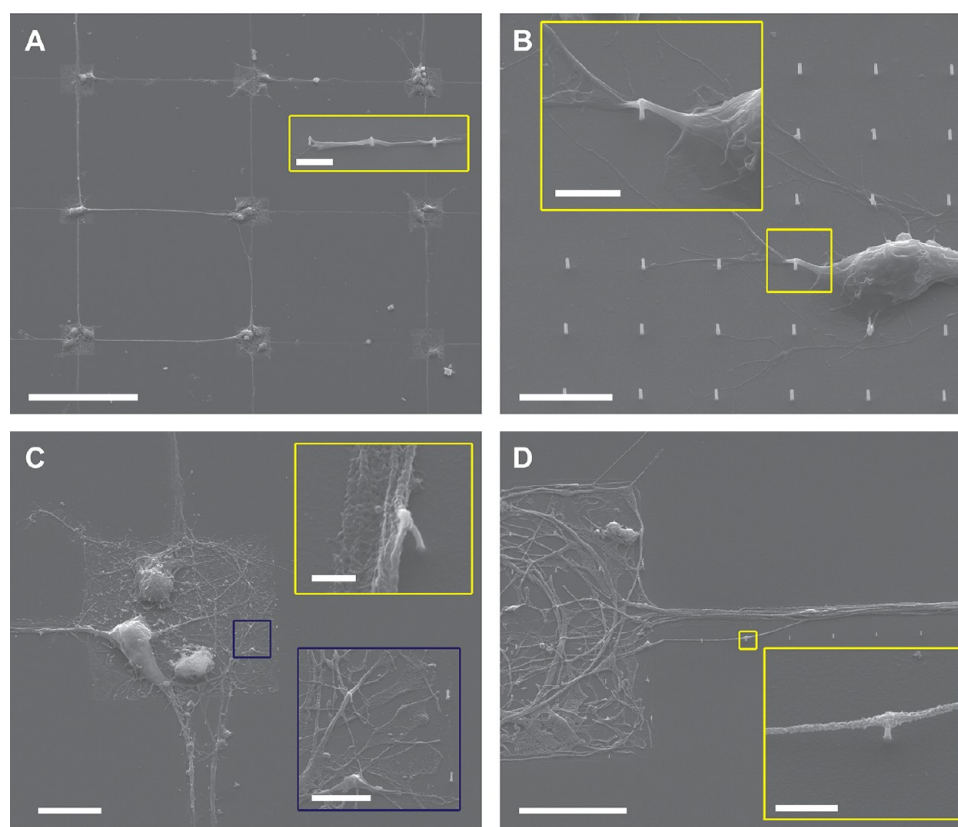


Figure 4. SEM images of cortical neuron cells, glia free, grown on Si pillars (70–100 nm diameter, 1 μm height, spaced 4 μm apart) arranged in a pattern of squares and lines that were chemically modified with fluorosilane and polylysine according to their pattern. (A) Network of cells grown in registration to the pillars. Inset shows zoom in picture of a neurite growing along the pillars, tightly wrapping them. Scale bars are 100 and 2.5 μm , respectively. (B) Single cell growing in a square. Inset is a zoom-in of the boxed area. Scale bars are 5 and 2 μm , respectively. (C) Close up on a patterned pillars-square. Yellow inset shows a neurite bending a pillar along the patterned-line. Blue inset is a zoom-in inside the square showing neurites growing atop the pillars. Scales bars are 10, 0.5, and 2.5 μm , respectively. (D) Floating neurite, growing atop a pillar. Inset shows zoom-in on the boxed area. Scale bars are 10 and 1 μm , respectively. All images were taken with 70° tilt.

allowing us to obtain controlled neuron growth with individual neurons crossing the NWs, and in the same time, connected to each other, forming a controlled network (Figure 5). Rat cortical neuron cell growth with the exclusion of glia cells was chemically guided with respect to the device elements in various geometrical configurations, creating artificial patterns designed to our will (Figure S3). This task is intriguing also because of the difficulty of culturing cells while maintaining good device characteristics; whereas on the other hand, cells can suffer from cytotoxicity caused by diffusion from the electrodes.⁵⁵ Nevertheless, cells were successfully maintained on these FET devices for a period of a week and sometimes more. In a former study,⁶⁴ a chemical pattern was used in order to spatially locate nanowire FET arrays along the axons, dendrites or at the junction with the cell body of single neuronal cells, however not with a complete connected network of cells like in here. In this setup, action potential spikes will be elicited using a conventional glass microelectrode at one cell while recording the conductance at the nanowire FET along its neighboring cells. This will allow studying of the propagation rate across a pre-defined distance between bursting neurons simultaneously coupled with the electrical properties of their sub-cellular compartments. Furthermore, chemical modification of these 3D-nanowire electrical devices will grant control over the incorporation of nanowire elements into the cells during the cellular growth process. Thus, 'nanowire-swallowed' elements will be used as intracellular electrical

sensors as well as chemical sensors for the simultaneous electrical and chemical monitoring of cell activity. In addition, nanowires could be used as neuron stimulators providing local potentials on the axons, dendrites and soma. Potentially, this setup will lead to intracellular electrical characterization of the complete dynamics of a network.

These achievements highlight the unique power of merging nanowire-based nanoelectronics with neuroscience, in hope to shed light on some fundamental questions on the intrinsic behavior of neuronal cells.

CONCLUSIONS

Developing new methods for using artificial, prepatterned neuronal networks *in vitro* holds a great promise for studying the development and dynamics of small neural systems. The primary purpose of the method described here is to produce highly ordered, mature and functional artificial mammalian neuronal networks, glia-free, that are maintained at low densities down to single cells. *In vitro* study of neuron activity favors the establishment of a one-to-one electrode-neuron correspondence,²⁷ therefore we consider our main achievement to be the answer for the essential and non trivial matters involving it. Hence, this protocol fulfills core requirement for a variety of applications that are bound to provide novel and important insights into the field of neurobiology, as demonstrated by its application on 3D-nano-pillars and 3D

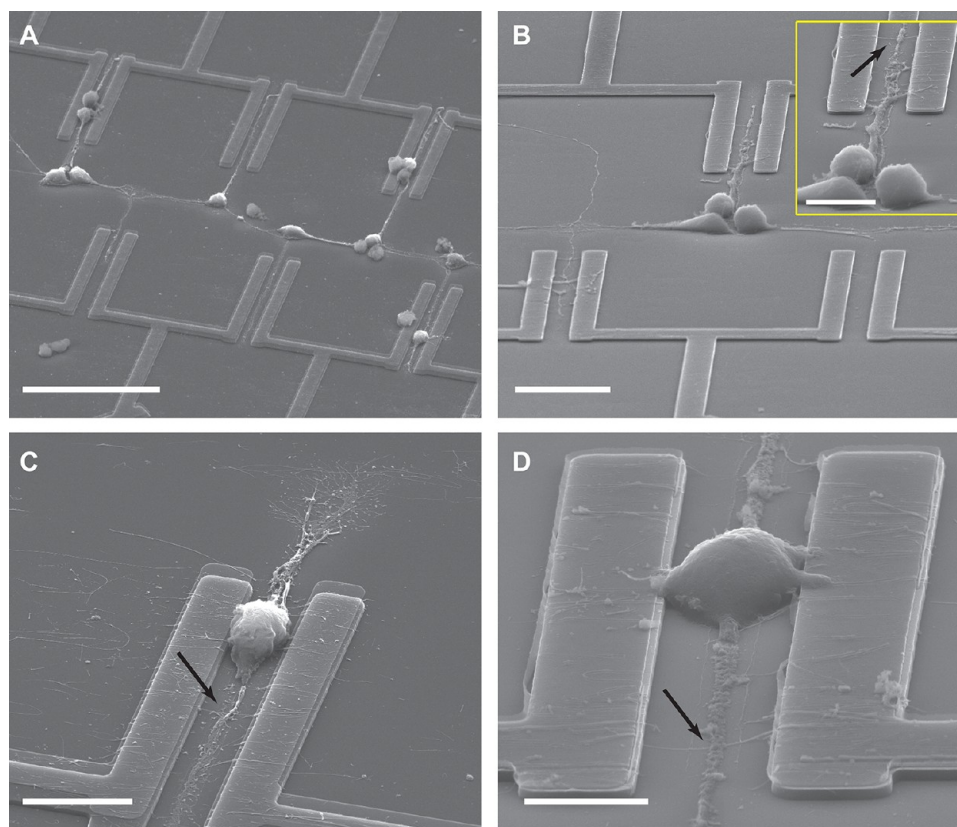


Figure 5. SEM images of controlled neuron growth, glia free, on SiNWs-FET devices in different geometrical configurations according to chemical guidance of fluorosilane and polylysine. (A) Configuration of a network grown at precise locations in registration to the NW FET-devices, with the neurites crossing the nanowire. Scale bar is 50 μm . (B) Close-up on a network configuration. Inset shows zoom in on a neurite crossing a NW (indicated by arrow). Scale bars are 20 and 10 μm , respectively. (C, D) Configuration of single cells with the soma region located between the source-drain electrodes. The arrows indicate a neurite crossing a NW. Scale bars are 10 and 5 μm , respectively.

nanowire-device arrays. There is opportunity for neurobiology to develop based on methods of SAMs, microfabrication, and nanoelectronic-based devices, setting new tools for patterning neurons and electrically stimulating them, while simultaneously detecting their cellular responses.⁶⁵ The technology is available; what remains is the integration of the relevant tools and their implementation.

EXPERIMENTAL SECTION

Chemical Surface Modification for Pattern Formation on SiO₂ Substrates (wafers, FET-devices, glass substrates). Prior to the chemical modification, samples were cleaned by oxygen plasma treatment: 100 W, 0.2 Torr O₂ for 200 sec. (1) Cleaned substrates were first modified with 1% (heptadecafluoro-1,1,2,2-tetrahydrodecyl) dimethylchlorosilane (cat. no. SIH5840.4, Gelest) in extra dry DCM/heptane (Biolab Ltd., Israel) 1:1 solution for 1 h at a clean room with low humidity atmosphere. Samples were immediately rinsed with DCM for 30 seconds followed by a curing step at 110 °C for 10 min, washed with acetone, and blown dry with N₂. (2) Samples were spin coated with Shipley 1818 (4000 rpm for 40 seconds) followed by baking at 115 °C on a hot plate for 5 min. Pattern was defined by photolithography (wavelength 400 nm, exposure time 5 s, AB-M 2130-C2 mask aligner) using a photomask. Pattern of squares and lines was set to be at sizes of 30 μm or 50 μm diameter squares with interconnecting lines of 2 μm width and 100 μm length to allow neurites elongation. Exposed samples were then developed in MF319 developer (Shipley) for 2.5 min with gentle agitation, and rinsed in dH₂O for another min. (3) Samples were cleaned using oxygen plasma (50W, 0.2 Torr O₂ for 4 min) to remove the fluorosilane layer only in the exposed areas. (4) Samples were soaked with 0.16 mg/mL poly-D-

lysine (PDL) hydrobromide (P7280, Sigma) over night. Excess of PDL was rinsed by repetitive washes in ddH₂O and dried in biological hood. (5) Lastly, photoresist was removed by short sonication in acetone and sequential washes in acetone, and substrates were sterilized by ethanol washing or autoclave. Cells were plated immediately after the chemical modification was completed.

Preparation of Neurons for Culturing on the Substrates. E18 primary cortical or hippocampal cells from Sprague/Dawley rat brain (99.9% glia-free) were shipped and provided as fresh microsurgically dissected tissue in a nutrient rich medium under refrigeration (cat. no N200200 and N100200, respectively, Genlantis). A protocol for cells dissection is given by Genlantis company and can be found on the net at: http://www.genlantis.com/objects/catalog/product/extras/1286_N200200_NeuroPure_E18_Cortical_Cells_MV14MAR2007.pdf.

However, we have conducted several changes in it as follows: cells were suspended in the provided plating medium (cat. no. N100100, Genlantis) with plating density of $\sim 1 \times 10^5$ cells/ml. The center area of each substrate was covered with 200 μl cell solution (~ 200 cells/ mm^2) and immediately put in the incubator for 1–1.5 h for cell attachment. Then, half of the plating media was taken out while simultaneously 2 ml of fresh warmed growing media (neurobasal media, 2% B27 serum free supplement, 1% glutamax and 1% pen-strep) were added into the plate to produce a final concentration of about 1000 cells per cm^2 . Samples were taken back into the incubator for another 1/2 to 1 h. Lastly, each substrate was covered with a standard sterile glass coverslip in order to protect the cells from oxidative stress. The combination of a serum free, chemically defined medium and culture in a sandwich configuration allows 80% greater survival of neurons.⁹ Cells were grown at 37 °C and 5% CO₂ with half of the medium replaced once a week. A viability assay with Trypan blue was used for evaluation of the cells viability prior to the cells plating and during

their growth. In addition, Live/Dead Viability/Cytotoxicity Kit for mammalian cells (Molecular Probes cat#L3224) was used as a cell viability assay to determine the percentage of living cells on control samples.

Electrophysiology. Cultures were studied at room temperature after 9 days. Current-clamp recordings were performed in glass cultured hippocampal neurons, using the whole-cell configuration of the patch-clamp technique. Patch clamp records were performed using Axopatch 200B and Digidata 1322A data acquisition interface, sampled at 5 kHz and filtered at 2 kHz via a 4-pole Bessel low pass filter. Bath solution contained in mM 150 NaCl, 2.5 KCl, 2 CaCl₂, 2 MgCl₂, 15 glucose, 10 Hepes, adjusted to pH to 7.4 and osmolarity to 325 mOsm. Pipette solution contained in mM 135 KCl, 1 MgATP, 2 EGTA, 1.1 CaCl₂, 5 glucose, 10 Hepes, adjusted to pH to 7.4 and osmolarity to 315 mOsm. Patch pipettes were made of standard borosilicate micropipets (Harvard Apparatus Company) and had a resistance of 4–7 MΩ when filled with the pipette solution. The series resistance was less than 15 MΩ, and was compensated up to 90% using a standard procedure. Resting membrane potentials were estimated directly after entering in whole cell configuration.

Si Pillar Fabrication. Si wafers were coated with MMA/PMMA resists (MicroChem) by spinning each at 5000 rpm for 60 sec and baking at 180° C for 3 min and 1 min, respectively. Pattern of 200 nm dot array and 4 μm spacing was written by e-beam lithography and metalized with 150 nm gold by e-beam evaporation. The remaining resist was removed with 1:1 acetone/isopropanol solution and blown dry using N₂ stream. Top-down vertical SiNWs arrays were fabricated by applying the Bosch RIE process in an ICP-DRIE PlasmaTherm SLR 770 machine. Briefly, alternated cycles of etching with SF₆ and passivation with C₄F₈ were used to etch the unprotected areas and to deposit fluorinated polymer to protect the side walls of the resulting etched structures; plasma was generated with an RF power of 600 W and platen power of 14 W at a pressure of 8 mTorr while maintaining the temperature at 22° C until a 1 μm height was achieved. After the formation of the nanowire arrays, the gold caps were chemically etched. Finally, reduction in diameter was performed by a dry thermal oxidation step at 850° C in an oxygen atmosphere at a pressure of 0.50 atm until 70–100 nm diameter was reached, followed by a short wet etching step in a BOE solution in order to remove the silicon oxide shell.

3D Suspended-SiNW Device Array Fabrication. First, reactive ion etching (RIE) was used to etch a Si substrate and create an elevated pattern of the contacts at a depth of ~400 nm. Then, SiNWs-FET devices were fabricated as previously described.⁶⁶ In short, p-type silicon nanowires of 20 nm diameter were synthesized by chemical vapor deposition by the vapor-liquid-solid (VLS) method. Source and drain electrodes were fabricated aligned to the elevated contacts-area by deposition of 300 nm LOR3A (Microchem) and 500 nm Shipley 1805 (Shipley). After exposure and development of the electrode patterns, contacts were metallized by e-beam and thermal evaporation of Ti/Pd/Ti (2/60/8 nm) respectively, and were passivated from the electrolyte with an insulating layer of Si₃N₄ (100 nm-thick) deposited by plasma-enhanced chemical vapor deposition (PECVD). The separation between the source and drain electrodes for each FET device was 6 μm. Prior to the chemical modification, chips were cleaned by oxygen plasma treatment of 30 W, 0.2 Torr O₂ for 60 s, and were ready for use.

Immunostaining and Confocal Microscope Imaging. The culture samples were fixated in 4% paraformaldehyde, 4% sucrose fixative in PBS, pH 7.4 for 20 min and permeabilized in 0.1% Triton X-100 for 10 min. Samples were then blocked with 4% BSA and 200 μg/mL Goat Gamma Globulin (Jackson Laboratories) in PBS for 30 min. Cultures were incubated with first antibodies over night at 4°c for labeling of axons (Tau 1:1000, Chemicon), dendrites (MAP2 1:2000, Chemicon), synapses (synaptophysin 1:500, Sigma) and glia cells (GFAP 1:200, CELL MARQUE). Secondary antibodies coupled to alexa fluor 488 and alexa fluor 594 (Invitrogen, cat. no A21202 and A21207) were used at dilutions of 1:250 for 30 min at room temp. Finally, nucleus was labeled with DAPI (Sigma) diluted 1:1000 for 10 min. Controls include incubations with no primary antibody. Confocal

images were obtained with a Leica SP5 confocal microscope. Images were acquired using excitation at 488 nm and 590 nm using LASAF software.

Sample Preparation for SEM Imaging. The culture samples were fixated in 4% paraformaldehyde/sucrose fixative, pH 7.4 for 20 min followed by a wash with PBS solution. Cultures were then dehydrated by rinsing in increasing ethanol concentrations of 25, 50, 75, 90, and 100% (×2), each time for 10 min. Finally, cells were dried with critical point dryer (Tousimis) and coated with Pd/Au via sputtering (Polaron). Samples were examined using a FEI QUANTA 200F scanning electron microscopy.

■ ASSOCIATED CONTENT

Supporting Information

This material is available free of charge via the Internet at <http://pubs.acs.org>.

■ AUTHOR INFORMATION

Corresponding Author

*E-mail: Fernando@post.tau.ac.il.

Notes

The authors declare no competing financial interest.

■ ACKNOWLEDGMENTS

This work was in part financially supported by the Legacy Fund-Israel Science Foundation (ISF) and the German-Israel Foundation (GIF).

■ REFERENCES

- (1) Yu, Z.; Xiang, G. X.; Pan, L. B.; Huang, L. H.; Yu, Z. Y.; Xing, W. L.; Cheng, J. *J. Biomed. Microdev.* **2004**, *6*, 311–324.
- (2) Kovacs, G. T. A. In *Enabling Technologies for Cultured Neural Networks*; Stenger, D. A., McKenna, T. M., Eds.; Academic Press: San Diego, 1994; pp 121–165.
- (3) Kim, D.-H.; Lee, H.; Lee, Y. K.; Nam, J.-M.; Levchenko, A. *Adv. Mater.* **2010**, *22*, 4551–4566.
- (4) Gupta, K.; Kim, D.-H.; Ellison, D.; Smith, C.; Kundu, A.; Tuan, J.; Suh, K.-Y.; Levchenko, A. *Lab Chip* **2010**, *10*, 2019–2031.
- (5) Kshitiz; Kim, D.-H.; Beebe, D. J.; Levchenko, A. *Trends Biotechnol.* **2011**, *29*, 399–408.
- (6) Goslin, K.; Banker, G. In *Culturing Nerve Cells*; Banker, G., Goslin, K., Eds.; MIT Press: Cambridge, MA, 1991; p 251–281.
- (7) Lo, Y. J.; Poo, M. M. *J. Neurosci.* **1994**, *14*, 4684–4693.
- (8) Kleinfeld, D.; Kahler, K. H.; Hockberger, P. E. *J. Neurosci.* **1988**, *8*, 4098–4120.
- (9) Brewer, G. J.; Cotman, C. W. *Brain Res.* **1989**, *494*, 65–74.
- (10) Brewer, G. J.; Torricelli, J. R.; Evege, E. K.; Price, P. J. *J. Neurosci. Res.* **1993**, *35*, 567–576.
- (11) Zhang, J.; Venkataramani, S.; Xu, H.; Song, Y.-K.; Song, H.-K.; Palmore, G. T. R.; Fallon, J.; Nurmikko, A. V. *Biomaterials* **2006**, *27*, 5734–5739.
- (12) Branch, D. W.; Corey, J. M.; Weyhenmeyer, J. A.; Brewer, G. J.; Wheeler, B. C. *Med. Biol. Eng. Comput.* **1998**, *36*, 135–141.
- (13) Wheeler, B. C.; Corey, J. M.; Brewer, G. J.; Branch, D. W. *J. Biomech. Eng.* **1999**, *121*, 73–78.
- (14) Branch, D. W.; Wheeler, B. C.; Brewer, G. J.; Leckband, D. E. *IEEE Trans. Biomed. Eng.* **2000**, *47*, 290–300.
- (15) Jun, S. B.; Hynd, M. R.; Dowell-Mesfin, N.; Smith, K. L.; Turner, J. N.; Shain, W.; Kim, S. J. *J. Neurosci. Methods* **2007**, *160*, 317–326.
- (16) Offenhausser, A.; Bocker-Meffert, S.; Decker, T.; Helpenstein, R.; Gasteier, P.; Groll, J.; Moller, M.; Reska, A.; Schafer, S.; Schulte, P.; Vogt-Eisele, A. *Soft Matter* **2007**, *3*, 290–298.
- (17) Liu, B.; Ma, J.; Gao, E.; He, Y.; Cui, F.; Xu, Q. *Biosens. Bioelectron.* **2008**, *23*, 1221–1228.
- (18) Lom, B.; Healy, K. E.; Hockberger, P. E. *J. Neurosci. Methods* **1993**, *50*, 385–397.

- (19) Wyart, C.; Ybert, C.; Bourdieu, L.; Herr, C.; Prinz, C.; Chatenay, D. *J. Neurosci. Methods* **2002**, *117*, 123–131.
- (20) Hammarback, J. A.; Palm, S. L.; Furcht, L. T.; Letourneau, P. C. *J. Neurosci. Res.* **1985**, *13*, 213–220.
- (21) Offenhausser, A.; Sprossler, C.; Matsuzawa, M.; Knoll, W. *Neurosci. Lett.* **1997**, *223*, 9–12.
- (22) Ma, W.; Liu, Q. Y.; Jung, D.; Manos, P.; Pancrazio, J. J.; Schaffner, A. E.; Barker, J. L.; Stenger, D. A. *Dev. Brain Res.* **1998**, *111*, 231–243.
- (23) Chang, J.; Wheeler, C. J. *Biomed. Microdev.* **2000**, *2*, 245.
- (24) Gross, G. W. *IEEE Trans. Biomed. Eng.* **1979**, *BME-26*, 273–279.
- (25) Jerome, P. J. *J. Neurosci. Methods* **1980**, *2*, 19–31.
- (26) Li, N.; Tourovskaja, A.; Folch, A. *Crit. Rev. Biomed. Eng.* **2003**, *31*, 423.
- (27) Yu, M.; Huang, Y.; Ballweg, J.; Shin, H.; Huang, M.; Savage, D. E.; Lagally, M. G.; Dent, E. W.; Blick, R. H.; Williams, J. C. *ACS Nano* **2011**, *5*, 2447–2457.
- (28) Ma, J.; Cui, F.; Liu, B.; Xu, Q. *J. Mater. Sci.: Mater. Med.* **2007**, *18*, 851–856.
- (29) Chang, J. C.; Brewer, G. J.; Wheeler, B. C. *J. Neural Eng.* **2006**, *3*, 217.
- (30) Xie, C.; Hanson, L.; Xie, W.; Lin, Z.; Cui, B.; Cui, Y. *Nano Lett.* **2010**, *10*, 4020–4024.
- (31) Fromherz, P. *Ann. N. Y. Acad. Sci.* **2006**, *1093*, 143–160.
- (32) Fromherz, P.; Offenhausser, A.; Vetter, T.; Weis, J. *Science* **1991**, *252*, 1290–1293.
- (33) Neves, G.; Cooke, S. F.; Bliss, T. V. P. *Nat. Rev. Neurosci.* **2008**, *9*, 65–75.
- (34) Hai, A.; Shappir, J.; Spira, M. E. *J. Neurophysiol.* **2010**, *104*, 559–568.
- (35) Voelker, M.; Fromherz, P. *Small* **2005**, *1*, 206–210.
- (36) Chang, W. C.; Sretavan, D. W. *Langmuir* **2008**, *24*, 13048–13057.
- (37) Sorribas, H.; Padeste, C.; Tiefenauer, L. *Biomaterials* **2002**, *23*, 893–900.
- (38) Lee, K.-Y.; Shim, S.; Kim, I.-S.; Oh, H.; Kim, S.; Ahn, J.-P.; Park, S.-H.; Rhim, H.; Choi, H.-J. *Nanoscale Res. Lett.* **2009**, *5*, 410–415.
- (39) Onclin, S.; Ravoo, B. J.; Reinhoudt, D. N. *Angew. Chem., Int. Ed.* **2005**, *44*, 6282–6304.
- (40) Navone, F. J., R.; Gioia, G. D.; Stukenbrok, H.; Greengard, P.; Camilli, P. D. *J. Cell Biol.* **1986**, *103*, 2511–2527.
- (41) Gao, Y.; Bhattacharya, S.; Chen, X.; Barizuddin, S.; Gangopadhyay, S.; Gillis, K. D. *Lab Chip* **2009**, *9*, 3442–3446.
- (42) Ahmet, B.; Sotoudeh, H.-H. *Nanotechnology* **2007**, *18*, 095201.
- (43) Patolsky, F.; Timko, B. P.; Zheng, G.; Lieber, C. M. *Mater. Res. Soc. Bull.* **2007**, *32*, 142–149.
- (44) Fan, R.; Wu, Y.; Li, D.; Yue, M.; Majumdar, A.; Yang, P. *J. Am. Chem. Soc.* **2003**, *125*, 5254–5255.
- (45) Hai, A.; Shappir, J.; Spira, M. E. *Nat. Methods* **2010**, *7*, 200–202.
- (46) Hällström, W.; Mårtensson, T.; Prinz, C.; Gustavsson, P.; Montelius, L.; Samuelson, L.; Kanje, M. *Nano Lett.* **2007**, *7*, 2960–2965.
- (47) Kim, W.; Ng, J. K.; Kunitake, M. E.; Conklin, B. R.; Yang, P. *J. Am. Chem. Soc.* **2007**, *129*, 7228–7229.
- (48) Jiang, K.; Fan, D.; Belabassi, Y.; Akkaraju, G.; Montchamp, J.-L.; Coffer, J. L. *ACS Appl. Mater. Interfaces* **2008**, *1*, 266–269.
- (49) Shalek, A. K.; Robinson, J. T.; Karp, E. S.; Lee, J. S.; Ahn, D.-R.; Yoon, M.-H.; Sutton, A.; Jorgolli, M.; Gertner, R. S.; Gujral, T. S.; MacBeath, G.; Yang, E. G.; Park, H. *Proc. Natl. Acad. Sci.* **2010**, *107*, 1870–1875.
- (50) Tian, B.; Cohen-Karni, T.; Qing, Q.; Duan, X.; Xie, P.; Lieber, C. M. *Science* **2010**, *329*, 830–834.
- (51) Patolsky, F.; Timko, B. P.; Yu, G.; Fang, Y.; Greytak, A. B.; Zheng, G.; Lieber, C. M. *Science* **2006**, *313*, 1100–4.
- (52) Qing, Q.; Pal, S. K.; Tian, B.; Duan, X.; Timko, B. P.; Cohen-Karni, T.; Murthy, V. N.; Lieber, C. M. *Proc. Natl. Acad. Sci.* **2010**, *107*, 1882–1887.
- (53) Xie, C.; Lin, Z.; Hanson, L.; Cui, Y.; Cui, B. *Nat. Nanotechnol.* **2012**, *7*, 185–190.
- (54) Duan, X.; Gao, R.; Xie, P.; Cohen-Karni, T.; Qing, Q.; Choe, H. S.; Tian, B.; Jiang, X.; Lieber, C. M. *Nat. Nanotechnol.* **2012**, *7*, 174–179.
- (55) Huys, R.; Braeken, D.; Van Meerbergen, B.; Winters, K.; Eberle, W.; Loo, J.; Tsvetanova, D.; Chen, C.; Severi, S.; Yitzchaik, S.; Spira, M.; Shappir, J.; Callewaert, G.; Borghs, G.; Bartic, C. *Solid-State Electron.* **2008**, *52*, 533–539.
- (56) Robinson, J. T.; Jorgolli, M.; Shalek, A. K.; Yoon, M.-H.; Gertner, R. S.; Park, H. *Nat. Nanotechnol.* **2012**, *7*, 180–184.
- (57) Hai, A.; Kamber, D.; Malkinson, G.; Erez, H.; Mazurski, N.; Shappir, J.; Spira, M. E. *J. Neural Eng.* **2009**, *6*, 066009.
- (58) Lim, J. Y.; Donahue, H. J. *Tissue Eng.* **2007**, *13*, 1879–91.
- (59) Wrobel, G.; Höller, M.; Ingebrandt, S.; Dieluweit, S.; Sommerhage, F.; Bochem, H. P.; Offenhausser, A. *J. R. Soc. Interface* **2008**, *5*, 213–222.
- (60) Sniadecki, N.; Desai, R.; Ruiz, S.; Chen, C. *Ann. Biomed. Eng.* **2006**, *34*, 59–74.
- (61) Spatz, J. P.; Geiger, B. *Methods Cell Biol.* **2007**, *83*, 89–111.
- (62) Keefer, E. W.; Botterman, B. R.; Romero, M. I.; Rossi, A. F.; Gross, G. W. *Nat. Nanotechnol.* **2008**, *3*, 434–439.
- (63) Shein, M.; Greenbaum, A.; Gabay, T.; Sorkin, R.; David-Pur, M.; Ben-Jacob, E.; Hanein, Y. *J. Biomed. Microdev.* **2009**, *11*, 495–501.
- (64) Patolsky, F.; Timko, B. P.; Yu, G. H.; Fang, Y.; Greytak, A. B.; Zheng, G. F.; Lieber, C. M. *Science* **2006**, *313*, 1100–1104.
- (65) Weibel, D. B.; Garstecki, P.; Whitesides, G. M. *Curr. Opin. Neurobiol.* **2005**, *15*, 560–567.
- (66) Patolsky, F.; Zheng, G.; Lieber, C. M. *Nat. Protocols* **2006**, *1*, 1711–1724.